NANO LETTERS

2007
Vol. 7, No. 6
1670−1675

Simulations and Analysis of Self-Assembly of CdTe Nanoparticles into Wires and Sheets

Zhenli Zhang,[†] Zhiyong Tang,[‡] Nicholas A. Kotov,[†,§,||] and Sharon C. Glotzer*[,†,§]

Department of Chemical Engineering, University of Michigan, Ann Arbor, Michigan 48109-2136, National Center for Nanoscience and Technology, Beijing 100080, China, Department of Materials Science and Engineering, University of Michigan, Ann Arbor, Michigan 48109-2136, and Department of Biomedical Engineering, University of Michigan, Ann Arbor, Michigan 48109-2136

Received March 16, 2007; Revised Manuscript Received April 18, 2007

ABSTRACT

Recent experiments have reported the self-assembly of TGA- and DMAET-stabilized CdTe nanoparticles (NPs) into wires and sheets, respectively, depending upon the stabilizer used. We develop a mesoscale model based on quantum mechanical calculations and perform Monte Carlo simulations of these NPs to elucidate the conditions under which these two structures will form. We show that consideration of NP shape, directional attraction, and electrostatic interactions is key to determining the anisotropy of the NP–NP interaction and final self-assembled structures.

Semiconductor nanoparticles (NPs), also known as quantum dots, show strongly size-, shape-, and composition-dependent photonic and electronic properties.[1] Individual NPs show great promise as nanoscale opto-electronic devices and for in vivo imaging and diagnostics for living cells.[2] The present challenge is assembling individual NPs into the desired nanostructures that have potential applications in novel functional nanodevices. Inspired by the complexity of protein suprastructures in biological systems, self-assembly of NPs through intrinsic NP−NP interactions is receiving increasing attention because of the size and interaction similarity between NPs and proteins and the growing ability to create NPs with anisotropic interactions. Despite some progress, this field is still in its infancy.[3] Rational biomimetic design of nanostructures remains an outstanding goal. One of the major challenges is that the relationship between NP−NP interactions and the resulting self-assembled nanostructures is not well understood and the controlling thermodynamic and kinetic factors that govern these self-assembly processes are not clear. The exploration of NP interactions is not only crucial to gain rational control over NP assemblies but also provides, indirectly, insight into the mechanism underlying the formation of protein superstructures in biological systems.

* Corresponding author. E-mail: sglotzer@umich.edu.
[†] Department of Chemical Engineering, University of Michigan.
[‡] National Center for Nanoscience and Technology.
[§] Department of Materials Science and Engineering, University of Michigan.
[||] Department of Biomedical Engineering, University of Michigan.

10.1021/nl0706300 CCC: $37.00
Published on Web 05/11/2007

In this paper, a CdTe NP system is used as a model system to study the effect of NP−NP interactions on the self-assembled structures that form spontaneously in aqueous solution. Recent experiments show that, by controlling the types of stabilizers on the NP surface, CdTe NPs can self-assemble into one-dimensional (1D) wires or two-dimensional sheets (2D) when the stabilizers used are thioglycolic acid molecules (hereafter referred to as the TGA−CdTe system) or 2-(dimethylamino)ethanethiol molecules (hereafter referred to as the DMAET−CdTe system), respectively.[4,5] In a recent paper, we showed using simulation that the sheets formed from a combination of anisotropic interactions arising from hydrophobic attractions and electrostatic interactions.[5] Why 1D wire structures form rather than sheets when TGA rather than DMAET is used as the stabilizer remains an open question, one that exemplifies that type of information needed to control NP assemblies. Here we answer this question by investigating the role of net charge, dipole directions, and NP concentration. We demonstrate that it is the negative net charge and the weak attractions of TGA−CdTe NPs that result in the formation of 1D wires.

Model and Simulation Method. Self-assembly of NPs involves multiple time scales and length scales. We utilize the results of quantum mechanical calculations to construct a mesoscale model for NP assembly.

Quantum Mechanics Calculations. Experiments have shown that the CdTe NPs in both TGA−CdTe and DMAET−

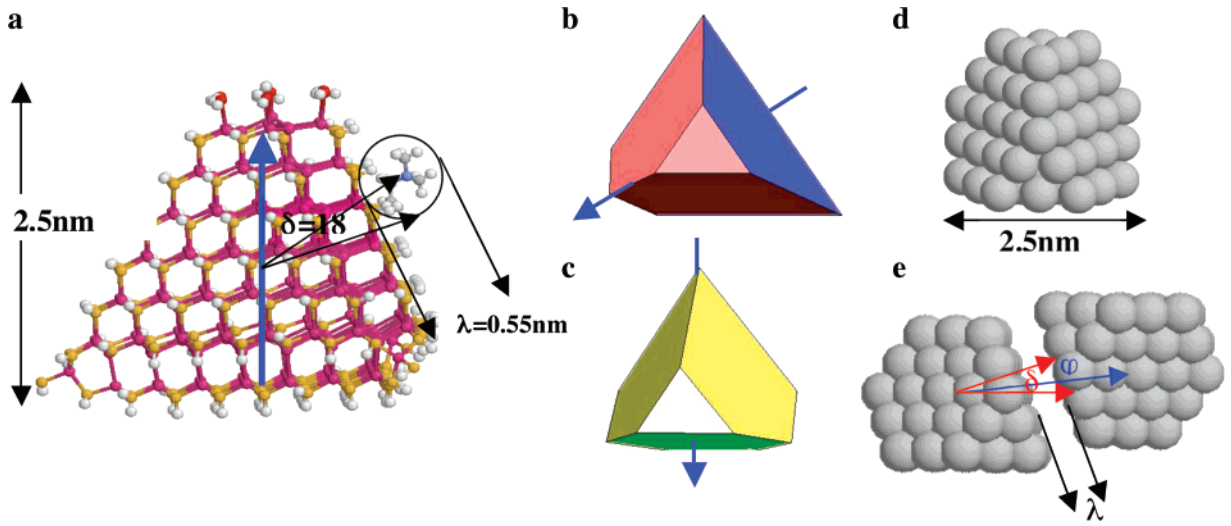

Figure 1. Quantum calculations and mesoscale simulation model. (a) Semiempirical quantum calculation of a single CdTe NP with one truncation. (b) Dipole direction of CdTe NP with two truncations, from QM calculations. (c) Dipole direction of CdTe NP with three truncations, from QM calculations. (d) Hard sphere model for NP. (e) Schematic illustration of directional attraction.

Table 1. Dipole Moment of a Single CdTe NP Calculated by Semiempirical PM3 Quantum Calculation by Spartan V4[a]

		N_T 1		N_T 2		N_T 3		N_T 4	
S_T		small	large	small	large	small	large	small	large
μ	SH	35.0 ± 8.8	86.9 ± 17.2	41.4 ± 7.8	78.4 ± 11.3	58.6 ± 4.3	77.6 ± 6.8	9.8 ± 0.4	9.8 ± 3.3
	H_2O	55.0 ± 4.8	57.8 ± 5.5	116.3 ± 5.6	115.2 ± 4.6	118.0 ± 7.0	184.6 ± 4.0	8.1 ± 2.7	5.7 ± 1.3

[a] The studied NP size is chosen to be 2.5 nm as Figure 1a illustrates. N_T is the number of truncations. S_T is the truncation size. "Small" represents two layers are cut in the truncated corners. "Large" represents three layers are cut. μ is the calculated dipole moment. Two types of NP surface patterns that affect the dipole moment are studied. In one, denoted by "SH", the NP is covered by SH groups as a minimal model for the stabilizers. In the other, denoted by "H_2O", the faces are coated with SH groups, but the truncated corners are covered by water molecules.

CdTe systems have a zinc blend crystal structure and possess a dipole moment.[4,5] Unlike in wurtzite semiconductors, the origin of the dipole moment in zinc blend structures is not apparent because they are considered to crystallize predominantly as tetrahedrons, which have no polar axis in the crystal lattice. The apparent discrepancy with the symmetry of the tetrahedron can be explained by assuming that the nanocrystals have the shape of a truncated tetrahedron. The high-energy apexes of the tetrahedron are likely to be replaced with less energetic crystal planes in NPs.[1,6] Because there are four apexes, some of them may be truncated and some of them may remain. Here we use semiempirical PM3 quantum mechanics calculations with Spartan V4 to study the dipole moment of CdTe NPs with 1, 2, 3, and 4 truncated corners. In addition to the number of truncated corners, we also consider other contributions to the dipole moment such as the size of the truncation and the stabilizer distribution on the NP surface.

Figure 1a shows the quantum calculation results for a single NP with one truncation. We term the face surrounded by the three untruncated corners as "bottom" and the other three faces as "side". For all cases we investigated, our calculations predict that the dipole direction points from the bottom to the truncated corner (Figure 1a). In contrast, for NPs with two truncations, the dipole points from the long edge to the opposite short edge (Figure 1b), and for NPs with three truncations, the dipole moment points from the opposite truncated corner to the bottom (Figure 1c). Table 1 summarizes the dependence of the dipole moment on the number of truncations, truncation size, and surface pattern. We find that the direction of the dipole moment is strongly dependent on the number of truncations, but only weakly dependent on surface pattern and truncation size. We further find the magnitude of the dipole moment varies from ~40 to ~180 Debye, which is generally consistent with known experimental values and theoretical predictions.[4,7]

Mesoscale Model. To investigate NP assembly, we construct a minimal model that contains only essential interactions. We first consider the forces acting between CdTe NPs. In the TGA−CdTe system, the TGA molecules confer a net negative charge to the NPs due to the ionization of the carboxyl groups. Additionally, van der Waals interactions and hydrogen bonds between TGA molecules cause an attraction between NPs.[4] In contrast, in the DMAET−CdTe system, the ionization of amino groups on the DMAET stabilizers confers a net positive charge to the NPs and the dimethyl groups of the DMAET molecules cause strong hydrophobic attractions between NPs.[5]

To simplify the model, we classify all types of interactions between NPs into three categories: (1) Excluded volume interactions; the unique truncated tetrahedral shape of CdTe NPs strongly influences their local packing.[8,9] (2) Directional short-ranged attractions; for TGA−CdTe NPs, the attractions come from van der Waals interactions and hydrogen bonding between TGA stabilizers. For DMAET−CdTe NPs, the attractions arise from hydrophobic attractions between

DMAET molecules. The directionality of the attraction arises from the relatively short length of the stabilizers and the nonspherical shape of the NPs. (3) Anisotropic electrostatic interactions; these arise for both systems due to the net charge conferred by the stabilizers and the dipole moment arising from truncation and stabilizers distribution on the NP surface.

To consider the excluded volume interactions, we use our previous patchy particle model[10] in which 58 hard, spherical beads are linked permanently together into a truncated tetrahedron (Figure 1d). The diameter of beads σ is chosen to be 0.5 nm, which corresponds to a typical NP size 2.5 nm shown in Figure 1d, intermediate in range between the experimental values of 2 and 5 nm. We assume four truncated corners based on the following argument. In experiments, the number of truncations of NPs likely varies and 0−4 truncations are all possible. However, four truncated corners should be the most likely because it is more energetically favorable than one, two, or three truncated corners. Although we have shown that NPs with four truncated corners possess no intrinsic dipole moment due to their symmetric shape, experiments indicate that they may acquire an induced dipole moment from their neighboring NPs that have asymmetric truncations and intrinsic strong dipole moments.[11,12]

The directional short-ranged attraction between NPs is modeled by a hard sphere, square-well potential modulated by an angular term (Figure 1e),[13]

$$U_{ij}(r_{ij};\mathbf{Q}_i,\mathbf{Q}_j) = u^{\mathrm{hssw}}(r_{ij})\cdot f(\mathbf{Q}_i,\mathbf{Q}_j) \tag{1}$$

where u^{hssw} is the usual hard sphere square-well potential,

$$u^{\mathrm{hssw}}(r_{ij}) = \begin{cases} \infty & \text{for overlap} \\ -\xi & \text{for } r_{ij} < 2l + \lambda, \text{ non-overlap} \\ 0 & \text{for } r_{ij} \geq 2l + \lambda, \text{ non-overlap} \end{cases} \tag{2}$$

Here ξ is the depth of the square-well potential representing the strength of attraction, r_{ij} is the distance between the centers of mass of NP i and j,; l is the distance from the mass center of the NP to its face, and λ is the interaction range. The function $f(\mathbf{Q}_i,\mathbf{Q}_j) = 1$ only if NPs i and j are oriented so that the angle between the vector joining their mass centers and the normal vector of the crystal face is less than δ; otherwise $f(\mathbf{Q}_i,\mathbf{Q}_j) = 0$. The angle δ and interaction range λ in combination determine the directionality of the attraction between the faces of two NPs, which can be estimated by the length ratio of the stabilizer and NP. The stabilizer length is approximately 0.55 nm for both systems and δ is about 18°, as determined in previous molecular simulations[5] (Figure 1a). Thus, we chose $\lambda = 0.55$ nm and $\delta = 18°$ in simulations.

The anisotropy of the electrostatic interaction arises from both net charge and dipole direction. We note that it is the tetrahedral shape of the NP that causes a coupling effect between net charge and dipole moment. The orientation dependence of the interaction energy varies as the sign of the net charge changes. The electrostatic potential between two NPs U_{ij} is modeled by

$$U_{ij}(r_{ij}) = \frac{q_i q_j}{4\pi\epsilon_0\epsilon r_{ij}} e^{-kr_{ij}} C_0^2 + \frac{q_i\mu_j \cos\theta_j + q_j\mu_i \cos\theta_i}{4\pi\epsilon_0\epsilon r_{ij}^2} e^{-kr_{ij}} C_0 C_1 + \frac{\mu_i\mu_j}{4\pi\epsilon_0\epsilon r_{ij}^3} \{\cos\theta_i \cos\theta_j [2 + kr_{ij} + (kr_{ij})^2] + \sin\theta_i \sin\theta_j \cos(\phi_i - \phi_j)[1 + kr_{ij}]\} e^{-kr_{ij}} C_1^2 \tag{3}$$

which was proposed by Phillies for polyelectrolyte colloids and proteins in dilute solution.[14] In the above equation, $C_0 = e^{ka}/(1 + ka)$ and $C_1 = 3e^{ka}/(2 + 2ka + (ka)^2 + (1 + ka)/\ni)$. Here $\ni$ is the ratio of NP to solvent dielectric constants, q_i and q_j are the net charge carried by NP i and NP j, μ_i and μ_j are dipole moments, r_{ij} is the distance between two NPs, θ_i and θ_j are the angles of the dipole vector with respect to the vector connecting the centers of the NPs, where $0 < \theta < \pi$, φ_i and φ_j are dihedral angles describing the relative rotation of the dipoles, where $0 < \varphi < 2\pi$, $1/k$ is the Debye screening length, which is set to be 2.5 nm, ϵ_0 is the permittivity of vacuum, ϵ is the effective permittivity of the solvent (water), a is the radius of the NP (We set it as half of the NP size as an approximation, 1.25 nm), and the dipole moment is set to be 100 D, as suggested by both experiments and our calculations.

Simulation Method. We perform Monte Carlo (MC) simulations with constant number $N = 60$ NPs, constant volume V, and constant temperature $T = 25$ °C. Simulations are performed in a cubic box with periodic boundary conditions implemented in all three Cartesian directions. A MC step is defined as N attempts at moving the particles by either translation or rotation. Our simulations begin from a disordered state, which is obtained by running 3−5 million MC steps with attractive energy $\xi = 0$. Subsequently, ξ is gradually increased from zero to a value at which ordered structures are observed. For each system, 4−10 independent runs are performed to ensure we obtain equilibrium structures.

NPs have three possible dipole directions, as parts a, b, and c of Figure 1 illustrate, and have either positive or negative charges. This yields six possible combinations: N1, N2, N3, P1, P2, and P3, where "N" indicates negative charge, "P" indicates positive charge, "1" indicates a dipole direction from the bottom to the corner (Figure 1a), "2" indicates a dipole direction from the long edge to the opposite short edge (Figure 1b), and "3" indicates a dipole direction from the corner to the bottom (Figure 1c). By symmetry, N1 is identical to P3, and N3 is identical to P1. We therefore investigate the four combinations N1 (P3), N2, P2, and N3 (P1).

Results. *N1 (P3).* For this system, sheetlike structures are obtained at all three concentrations we investigated (ϕ = 0.11, 0.13, and 0.15) and for all the independent runs we performed. As an illustration, parts a and b of Figure 2 show the face view and side view of sheets obtained at $\phi = 0.11$. The face view of a single sheet illustrates that within the sheets, NPs form rings, which agrees with the experimental findings (Figure 2c). Each ring is comprised of six NPs, and every bottom-upward NP is adjacent to three corner-upward NPs and vice versa. To characterize the formation of sheets,

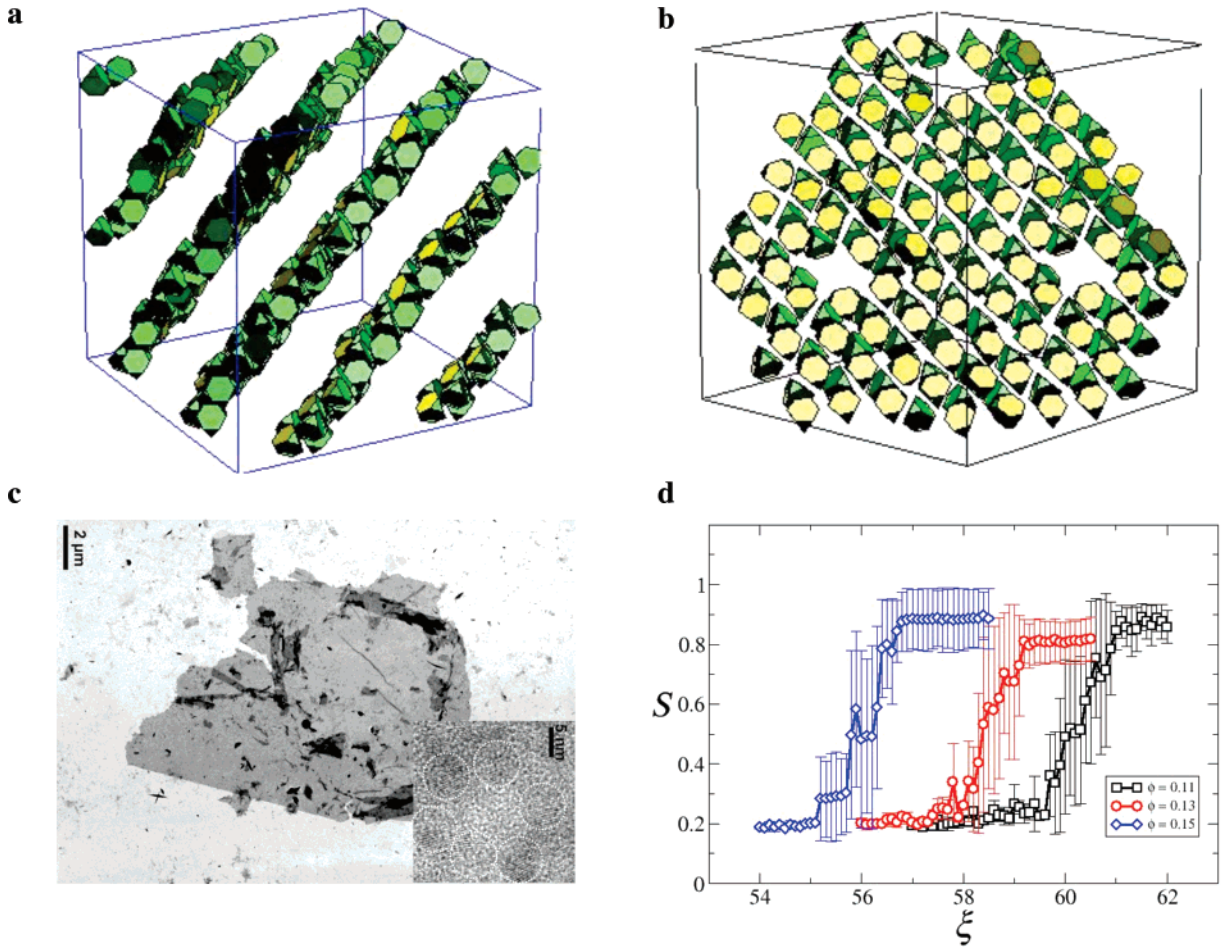

Figure 2. Mesoscale simulation results: sheet formation. (a) Side view of the sheets formed by system N1 (P3). (b) Face view of a single sheet in A. (c) TEM image of nanosheets formed by CdTe NPs with DMAET stabilizers. Inset is HRTEM image of nanosheets demonstrating the ringlike packing of NPs. (d) Dependence of order parameter on attraction strength at three concentrations.

we use a scalar order parameter, $S = (^3/_2\mathbf{S}:\mathbf{S})^{1/2}$. $\mathbf{S}$ is the orientational tensor defined by $\mathbf{S} = \langle\mathbf{uu}\rangle - {}^1/_3\mathbf{e}$, where $\mathbf{u}$ is the unit vector of the dipole moment and $\mathbf{e}$ is the unit tensor. The plots of S as a function of attraction strength ξ for three different concentrations are shown in Figure 2d. We see there is a clear transition when the sheets form. The value of ξ_c, which characterizes the critical attraction needed to form sheets, increases from 57 kJ/mol ($\phi = 0.15$) to 61 kJ/mol ($\phi = 0.11$) as the concentration decreases.

N2, P2. We obtain chain-like structures, or wires, for both N2 and P2, as demonstrated in Figure 3a,b (for visualization purposes only two wires are shown). The chainlike structure is confirmed by analysis of the coordination number. The analysis shows that NPs with two neighbors comprise the majority of the system (84.28 ± 4.44% for N2 and 84.30 ± 5.14% for P2). One major finding of our simulation is that NPs are arranged within wires in a face-to-face packing, which implies that the dipole directions are alternatively perpendicular to the wire axis. It should be noted that this is different from previous arguments that the dipoles are arranged head-to-tail,[4,15] as in chains of dipolar spheres.[16] The TEM image and inset HRTEM image in Figure 3c clearly demonstrate that the wires are kinked on the length scale of individual NPs, which supports our simulation results. Figure 3d shows the potential energy per particle as a function of attraction at three different concentrations for both systems. It demonstrates that the transition from disordered state to chains is smooth and it is almost the same for N2 and P2. The figure also indicates the formation of chains occurs when the NP attraction is greater than 43 kJ/mol, with slight variation with concentration. However, one major difference between N2 and P2 exists. In N2, the NP faces align near the positive part of the dipole (colored red in Figure 3a). However, in P2, the NP faces align near the negative part of the dipole (colored blue in Figure 3b). The reason for this will be discussed in the later analysis section.

N3 (P1). For this system, we obtain only small aggregates. Visually, we observe that most of the aggregates are dimers, which is confirmed by the fact that most of the NPs (74.22 ± 4.32%) have one neighbor. In the dimers, two NPs are observed to associate through a side-to-bottom alignment. This is confirmed by analysis of the orientation distribution of neighboring particles. The analysis shows that 73.33% of neighboring NPs are oriented in that way.

Analysis. Why does the difference in the sign of the charge and dipole direction leads to different self-assembled structures? To answer this question, we perform an energy analysis in which we consider relative potential energies and neglect entropic contributions. For two adjacent NPs, the potential energy varies with their relative orientation because

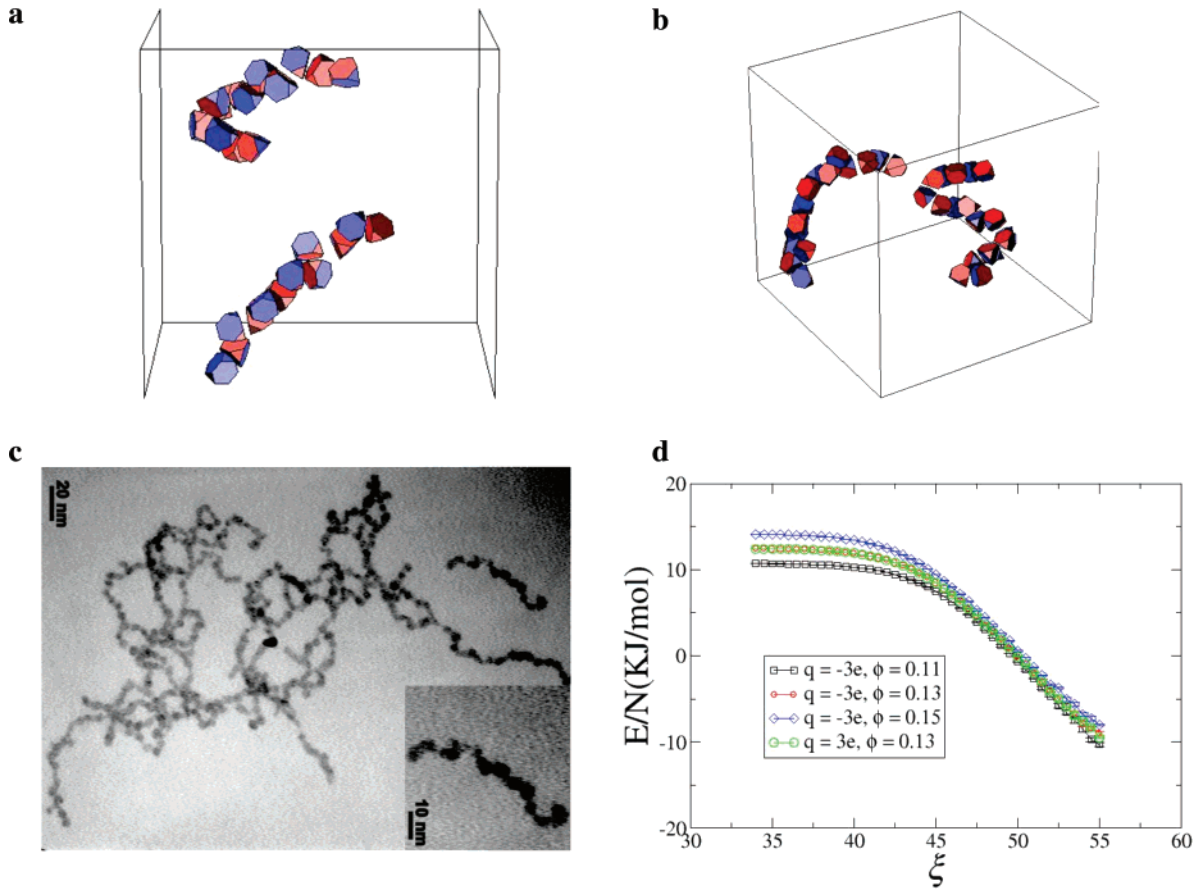

Figure 3. Mesoscale simulation results: chain formation. (a) The chains formed by system N2. (b) The chains formed by system P2. (c) TEM image of nanowires formed by CdTe NPs with TGA stabilizers. Inset image shows the kinked structure of the wires. (d) Potential energy as a function of attraction for systems N2 and P2.

Table 2. Electrostatic Energy of Two NPs as a Function of Relative Orientation for N2 and P2 (separation $r = 0.55$ nm)[a]

system (relative orientation)	N2(FN−FP), P2(FN−FP)				N2(FN−FN), P2(FP−FP)				N2(FP−FP), P2(FN−FN)			
	$\Delta\varphi = 0°$	$\Delta\varphi = 60°$	$\Delta\varphi = 120°$	$\Delta\varphi = 180°$	$\Delta\varphi = 0°$	$\Delta\varphi = 60°$	$\Delta\varphi = 120°$	$\Delta\varphi = 180°$	$\Delta\varphi = 0°$	$\Delta\varphi = 60°$	$\Delta\varphi = 120°$	$\Delta\varphi = 180°$
U_{qq}	53.47				53.47				53.47			
$U_{q\mu}$	0.00				26.34				−26.34			
$U_{\mu\mu}$	−0.74	−2.44	−5.83	−7.53	7.53	5.83	2.44	0.74	7.53	5.83	2.44	0.74
U_t	52.73	51.03	47.64	45.94	87.35	85.65	82.25	80.55	34.66	32.96	29.56	**27.86**

[a] U_{qq} is the charge−charge interaction, $U_{q\mu}$ is the charge−dipole interaction, $U_{\mu\mu}$ is the dipole−dipole interaction, and U_t is the total electrostatic interaction. All energy is in units of kJ/mol. $\Delta\varphi$ is the dihedral angle between the dipole directions of adjacent NPs. The lowest total electrostatic interaction energy is indicated in bold.

of the coupling of the charge and dipole interactions. Consider N2 and P2 as examples. The four faces of these particles may be classified into two types. The two faces adjacent to the long edge (see Figure 1b) are termed as "FN" (negative, blue). The other two faces are termed as "FP" (positive, red). Therefore, there are three types of associations: FN−FN, FN−FP, and FP−FP. To evaluate the potential energy, we should also consider the relative dihedral angle $\Delta\varphi$ of the dipoles for a given association. Table 2 shows the potential energy as a function of orientation for N2 and P2. We can see that the charge−dipole interactions are dominant and determine the favorable FP−FP local packing for N2 and FN−FN packing for P2 observed in our simulations. The energy analysis also agrees with the simulations that the lowest energy state is $\Delta\varphi = 180°$, and we find that the average $\Delta\varphi$ in simulations is 178°. We note that dipole−dipole interactions are usually assumed to be responsible for the one-dimensional self-assembly of nanoparticles in previous studies.[4,11,17] Instead, our simulations indicate that the charge−dipole interaction is the key factor. A similar energy analysis is performed for N1 (P3) and N3 (P1). Table 3 list the potential energy for N3 (P1) as a function of orientation. It is seen that the lowest energy is the bottom−bottom orientation. This type of association leads to the formation of dimers, which is consistent with the simulation results. Our previous analysis[5] demonstrated that, for N1 (P3), the lowest-energy state is instead the side−side association with $\Delta\varphi = 180°$, which favors sheet

Table 3. Electrostatic Energy of Two NPs as a Function of Relative Orientation for System N3 (P1)[a]

			side−side			
relative orientation	bottom−bottom	bottom−side	$\Delta\varphi = 0°$	$\Delta\varphi = 60°$	$\Delta\varphi = 120°$	$\Delta\varphi = 180°$
U_{qq}	53.47	53.47	53.47	53.47	53.47	53.47
$U_{q\mu}$	−45.63	−15.21	15.21	15.21	15.21	15.21
$U_{\mu\mu}$	12.40	−4.13	5.91	3.64	−0.89	−3.15
U_t	**20.24**	34.12	74.59	72.32	67.79	65.53

[a] The labels are as in Table 2. The lowest total electrostatic interaction energy is indicated in bold.

formation. Comparing these two cases, we can see that again it is the charge−dipole coupling interactions that differentiate the final assembled structures.

Discussion. The systems with negative charge (N1, N2, and N3) correspond to the TGA−CdTe system, and the systems with positive charge (P1, P2, and P3) correspond to the DMAET−CdTe system. Because both systems have the potential to form wires and sheets, as demonstrated by our mesoscale simulations, why is the TGA−CdTe system experimentally found to form only wires and the DMAET−CdTe system found to form only sheets?

In sheets, each NP has three neighbors that have directional attraction, while for wires and dimers, the numbers of neighbors are two and one, respectively. Therefore, for a given value of attraction ξ, the sheets have the lowest energy per particle (considering that the attraction is much stronger than the electrostatic interactions). The attractive energy per particle for the wires is higher than that for sheets, and it the highest for the dimers. Thus, from an energetic standpoint, NPs should choose to form sheets first and then wires. However, the formation of sheets requires two additional conditions. The first is the proper dipole direction. For NPs with positive charge (DMAET−CdTe), the dipole direction should be from the opposite corner to the bottom, which further implies that some NPs (those that induce dipole moments in fully truncated NPs) need to have three truncations. For NPs with negative charge (TGA−CdTe), the dipole direction should be from the bottom to a corner, which requires that some NPs have one truncation. Regardless of system, there are likely many more NPs with three truncations than those with one truncation because the former has lower energy. Thus it is not favorable for TGA−CdTe NPs to form sheets. The second condition is that the attraction be large enough to overcome electrostatic repulsion between like-charged NPs. To form sheets, the critical attraction (57 kJ/mol) is higher (maybe much higher when the concentration is very low) than that needed to form chains (43 kJ/mol). As we know, for the TGA−CdTe system, the stabilizers interact through van der Waals and hydrogen bonding, which is substantially weaker than hydrophobic attraction. Therefore, the attraction may be insufficient to form the sheets. In experiments, both factors may lead to the failure of TGA−CdTe NPs to form sheets and the formation, instead, of chains.

In conclusion, we have performed simulations of CdTe NPs on multiple scales to rationalize the self-assembled structures observed in recent experiments. Our simulations demonstrate that the delicate balance of various anisotropic interactions between NPs is responsible for the observed one-dimensional and two-dimensional assemblies. The particular energy landscape of NPs determines the specific local packing of NPs and finally leads to various global symmetry-broken structures. Consideration of NP shape, directional attraction, and electrostatic interactions is key to determining the anisotropy of the interaction and final self-assembled structures. It should be noted that proteins possess similar interactions and physical dimensions as these NBBs. The tertiary structures of proteins possess specific shape, nonuniform surface functional groups (e.g., hydrophobic and hydrophilic parts), net surface charges, and also intrinsic dipole (or multipole) moments. Because proteins self-assemble into diverse suprastructures, our simulations hopefully provide instructive views to understand these self-assembly processes in biological systems and provide an initial guideline for rationally controlling the biomimetic assembly of NPs.

Acknowledgment. Financial support for Z.L.Z. and S.C.G. was provided by the Department of Energy, under grant no. DE-FG02-02ER4600. Z.Y.T. thanks the 100-talent program of the Chinese Academy of Sciences for financial support. N.A.K. acknowledge financial support from NSF, grant no. 0601345.

References

(1) Alivisatos, A. P. *Science* **1996**, *271*, 933.
(2) Michalet, X.; Pinaud, F. F.; Bentolila, L. A.; Tsay, J. M.; Doose, S.; Li, J. J.; Sundaresan, G.; Wu, A. M.; Gambhir, S. S.; Weiss, S. *Science* **2005**, *307*, 538.
(3) Zhang, S. G. *Nat. Biotechnol.* **2003**, *21*, 1171.
(4) Tang, Z. Y.; Kotov, N. A.; Giersig, M. *Science* **2002**, *297*, 237.
(5) Tang, Z. Y.; Zhang, Z. L.; Wang, Y.; Glotzer, S. C.; Kotov, N. A. *Science* **2006**, *314*, 274.
(6) Wang, Z. L. *J. Phys. Chem. B* **2000**, *104*, 1153.
(7) Shim, M.; Guyot-Sionnest, P. *J. Chem. Phys.* **1999**, *111*, 6955.
(8) John, B. S.; Escobedo, F. A. *J. Phys. Chem. B* **2005**, *109*, 23008.
(9) Zhang, X.; Zhang, Z. L.; Glotzer, S. C. *J. Phys. Chem. C* **2007**, *111*, 4132.
(10) Zhang, Z. L.; Glotzer, S. C. *Nano Lett.* **2004**, *4*, 1407.
(11) Cho, K. S.; Talapin, D. V.; Gaschler, W.; Murray, C. B. *J. Am. Chem. Soc.* **2005**, *127*, 7140.
(12) Wang, F.; Shan, J.; Islam, M. A.; Herman, I. P.; Bonn, M.; Heinz, T. F. *Nat. Mater.* **2006**, *5*, 861.
(13) Wertheim, M. S. *J. Stat. Phys.* **1984**, *35*, 19.
(14) Phillies, G. D. *J. Chem. Phys.* **1974**, *60*, 2721.
(15) Sinyagin, A. Y.; Belov, A.; Tang, Z. Y.; Kotov, N. A. *J. Phys. Chem. B* **2006**, *110*, 7500.
(16) Teixeira, P. I. C.; Tavares, J. M.; da Gama, M. M. T. *J. Phys.: Condens. Matter* **2000**, *12*, R411.
(17) Wang, L.; Wei, G.; Sun, L. L.; Liu, Z. G.; Song, Y. H.; Yang, T.; Sun, Y. J.; Guo, C. L.; Li, Z. *Nanotechnology* **2006**, *17*, 2907.

NL0706300